

Solubility Measurement and Correlation of Itraconazole Hydroxy Isobutyltriazolone in Four Kinds of Binary Solvent Mixtures with Temperature from 283.15 to 323.15 K

Qi Dong,[§] Shuai Yu,[§] Xingzhu Wang, Shangzhi Ding, Enxia Li, Yuanxing Cai,* and Fumin Xue*



Cite This: ACS Omega 2023, 8, 39390–39400



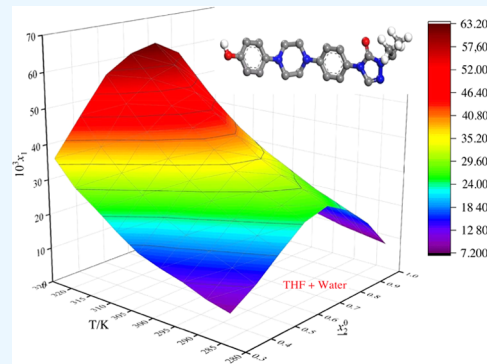
Read Online

ACCESS |

Metrics & More

Article Recommendations

ABSTRACT: The solubility of itraconazole hydroxy isobutyltriazolone (IHI) in four commonly used binary solvent mixtures of *N,N*-dimethylformamide (DMF) + water, DMF + ethanol, tetrahydrofuran (THF) + water, and THF + ethanol was determined with gravimetric method at temperatures ranging from 283.15 to 323.15 K under atmospheric pressure. The solubility of IHI in all selected solvents increases with the increase of temperature. The maximum solubility of IHI exists in the solvent of DMF + ethanol ($0.06523 \text{ mol}\cdot\text{mol}^{-1}$, $x_2^0 = 0.7$, $T = 323.15 \text{ K}$), while the minimum solubility exists in DMF + water ($0.0003723 \text{ mol}\cdot\text{mol}^{-1}$, $x_2^0 = 0.3$, $T = 283.15 \text{ K}$). There is a co-solvency phenomenon in the mixed solvents of DMF + ethanol, THF + water, and THF + ethanol. Four thermodynamic models, including the modified Apelblat model, the Yaws model, the Sun model, and the modified Jouyban–Acree model, were selected to fit the solubility data of IHI. All the RAD values are less than 0.0484, and RMSD values are not more than 0.001319. The Yaws model and the modified Apelblat model fit the solubility data of IHI better than the other two models. All the selected four models can fit the solubility data of IHI well.



1. INTRODUCTION

Itraconazole hydroxy isobutyltriazolone (chemical name: 2,4-Dihydro-4-[4-(4-hydroxyphenyl)-1-piperazinyl] phenyl]-2-

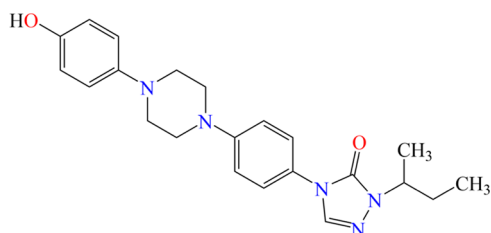


Figure 1. Chemical structure of IHI.

(1-methylpropyl)-3H-1,2,4-triazol-3-one, empirical formula: $\text{C}_{22}\text{H}_{27}\text{N}_5\text{O}_2$, CAS No. 106461-41-0, $M_W = 393.48 \text{ g}\cdot\text{mol}^{-1}$) is a dark white powder in crystalline form. Itraconazole hydroxy isobutyltriazolone (IHI for short) is almost insoluble in water.¹ The molecular structure of IHI is shown in Figure 1. IHI is an important medicine intermediate and has mainly been used as a medical intermediate of itraconazole.

Currently, there is little research on the crystallization process of IHI. Crystallization is the final step in the preparation of active pharmaceutical ingredients (API) and plays a crucial role in the properties of product particles. It is undeniable that solubility

data is required by the optimization of the crystallization process. Solubility data can guide the selection of solvent systems and crystallization methods (cooling crystallization, reaction crystallization, antisolvent crystallization, evaporation crystallization, etc.^{2,3}). Nevertheless, there is currently no detailed reference material on the solubility of IHI in pure or binary solvent systems.

In the field of pharmaceuticals, it can be used as a drug intermediate to produce Itraconazole. The solubility of IHI in four commonly used binary solvent mixtures of *N,N*-dimethylformamide (DMF) + water, DMF + ethanol, tetrahydrofuran (THF) + water, and THF + ethanol was determined. Previous studies have discussed the selection of binary solvents, such as solvents that are easily soluble in drugs as good solvents and solvents that are slightly soluble or insoluble in drugs as antisolvents.^{4–6} The static gravimetric method was selected to measure the solubility of IHI. The temperature ranges from 283.15 to 323.15 K (interval 5.0 K). The pressure is approximately 0.1 MPa. The solubility data were fitted by

Received: July 12, 2023

Accepted: July 27, 2023

Published: October 11, 2023



ACS Publications

Table 1. Detailed Information of Materials Used

chemicals	CAS no.	molar mass (g·mol ⁻¹)	mass fraction purity ^a	source
itraconazole hydroxy isobutyltriazolone (IHI)	106461-41-0	393.48	≥ 0.980	Aladdin Holdings Group Co., Ltd.
water	7732-18-5	18.02	ultrapure	produced in our laboratory
ethanol	64-17-5	46.07	≥ 0.997	Sinopharm Chemical Reagent Co., Ltd.
tetrahydrofuran	109-99-9	72.11	≥ 0.995	Fuyu Fine Chemical Co., Ltd.
N,N-dimethylformamide (DMF)	68-12-2	73.09	≥ 0.995	Fuyu Fine Chemical Co., Ltd.

^aBoth the analysis method and mass fraction purity were claimed by suppliers.

different thermodynamic models. These solubility data contain important practical significance for the optimization of the crystallization process of IHI and its corresponding industrial production.

Measuring the solubility of drugs in different solvents and temperatures not only helps to select appropriate solvents and temperatures for drug purification but also optimizes the crystallization process and improves the product quality of drugs, and the determination of solubility is of great significance.^{7,8}

2. THEORETICAL MODELS

With the aim of finding better models to correlate the solubility data of IHI in binary solvents and predicting the solubility data of IHI, different thermodynamic models were selected.^{9–11} In this investigation, four classical models, including the modified Apelblat model, the Yaws model, the Sun model, and the modified Jouyban–Acree model, were selected.

2.1. Modified Apelblat Model. The Apelblat model is a semiempirical model widely used to correlate the solubility data and temperature, which can be described as follows^{12–15}

$$\ln x_1 = A + \frac{B}{T} + C \ln T \quad (1)$$

where x_1 is the mole fraction of IHI, T is the absolute thermodynamic temperature, and A , B , and C are model parameters.

2.2. Yaws Model. Another semiempirical model, the Yaws model was also used to fit the solubility data. Just as the modified Apelblat model, it can also be used to correlate the solubility at different temperatures in mono solvents. On the right side of the equation, the form and meaning of the first two terms are similar to those of the expression of the modified Apelblat equation, while the third term can be helpful to improve the performance on describing some special varying tendencies of solubility data, which can be described as follows^{16–19}

$$\ln x_1 = E + \frac{F}{T} + \frac{G}{T^2} \quad (2)$$

2.3. Sun Model. The Sun model is used to correlate the solubility data at different temperatures and different compositions of mixed solvents, which can be described as follows²⁰

$$\begin{aligned} \ln x_1 = D_1 + \frac{D_2}{T} + D_3 x_2^0 + D_4 \frac{x_2^0}{T} + D_5 \frac{(x_2^0)^2}{T} + D_6 \frac{(x_2^0)^3}{T} \\ + D_7 \frac{(x_2^0)^4}{T} \end{aligned} \quad (3)$$

where D_1 to D_7 are the model parameters.

2.4. Modified Jouyban–Acree Model. The Jouyban–Acree model can be defined as^{21,22}

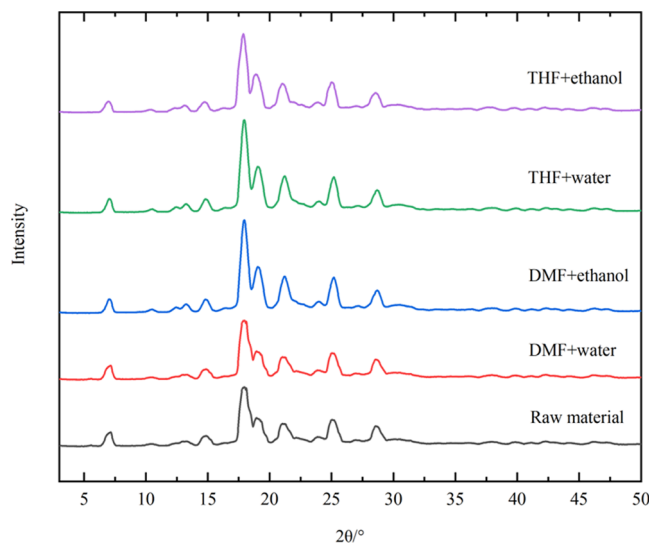


Figure 2. XRPD patterns of IHI raw material and IHI in different solid-liquid equilibrium systems ($x_2^0 = 0.6$).

$$\ln x_1 = x_2^0(x_1)_2 + x_3^0(x_1)_3 + x_2^0 x_3^0 \sum_{i=0}^N \frac{J_i(x_2^0 - x_3^0)^i}{T} \quad (4)$$

where x_1 , x_2^0 , and x_3^0 are the mole fractions of solute, good solvent, and antisolvent, respectively; T is the absolute temperature; N is the number of the solvents, which is equal to two for a binary solvent mixture; and J_i constitutes the model parameters. When combined with the modified Apelblat model, the modified Jouyban–Acree model can be obtained and expressed as follows²³

$$\begin{aligned} \ln x_1 = A_1 + \frac{A_2}{T} + A_3 \ln T + A_4 x_2^0 + A_5 \frac{x_2^0}{T} + A_6 \frac{(x_2^0)^2}{T} \\ + A_7 \frac{(x_2^0)^3}{T} + A_8 \frac{(x_2^0)^4}{T} + A_9 x_2^0 \ln T \end{aligned} \quad (5)$$

where A_1 to A_9 are the final model parameters.

2.5. Data Correlation. Relative average deviation (RAD) and root mean square deviation (RMSD) were selected to evaluate the fitting level of each model^{24–26}

$$\text{RAD} = \frac{1}{N} \sum_i^N \left| \frac{x_1^{\text{exp}} - x_1^{\text{cal}}}{x_1^{\text{exp}}} \right| \quad (6)$$

$$\text{RMSD} = \left[\frac{1}{N} \sum_i^N (x_1^{\text{cal}} - x_1^{\text{exp}})^2 \right]^{1/2} \quad (7)$$

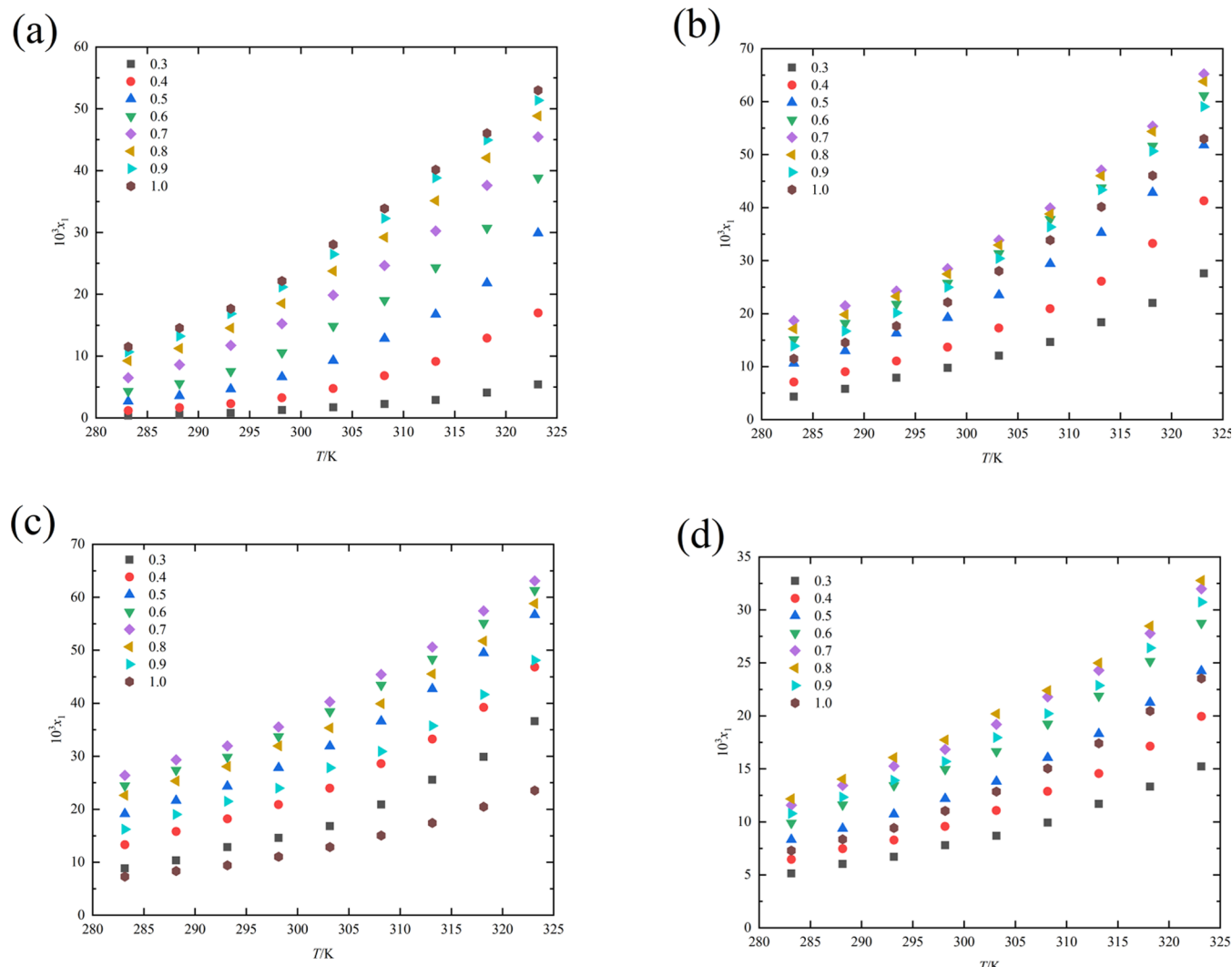


Figure 3. Mole fraction solubility of IHI in different binary mixed solvents: (a) DMF + water, (b) DMF + ethanol, (c) THF + water, and (d) THF + ethanol.

where x_1^{exp} and x_1^{cal} are the experimental and calculated solubility data, respectively, with N denoting the number of experimental points.

3. EXPERIMENTAL SECTION

3.1. Materials. Itraconazole hydroxy isobutyltriazolone (IHI, mass fraction 98%) was purchased from Aladdin Holdings Group Co., Ltd. Information about all of the solvents used in this investigation is listed in Table 1. The organic solvents (including ethanol, tetrahydrofuran, and *N,N*-dimethylformamide) were of analytical grade as purchased from Sinopharm Chemical Reagent Co., Ltd. or Fuyu Fine Chemical Co., Ltd. All of the solvents were used without further purification. Ultrapure water was produced in our laboratory (Arium Advance EDI, Sartorius, Germany).

3.2. X-ray Powder Diffraction. The residual solids of IHI in solubility measurement experiments in different solvent systems and raw materials were characterized using X-ray powder diffraction (XRPD). X'Pert3 Powder (PANalytical B.V., Netherlands) and Cu $\text{K}\alpha$ were used radiation together. The tube voltage is 40 kV, and the current is 30 mA. Under nitrogen environment protection, the testing range is 3–50° (2θ), and

the scanning speed is 8°/min. All measured temperatures and pressures were 298.15 K and 0.1 MPa, respectively.

3.3. Solubility Determination. A gravimetric method was selected to measure the solubility of IHI in four binary solvents (DMF + water, DMF + ethanol, THF + water, and THF + ethanol) at temperatures ranging from 283.15 to 323.15 K at 0.1 MPa. The measurement system used here has been widely used in our previous work.^{5,6,21} First, each pure solvent was accurately weighed into a beaker to prepare binary solvents with different antisolvent compositions. Then, approximately 150 mL of mixed solvents were added to a 200 mL volume glass jacketed container. A rubber stopper was used to minimize the evaporation of solvent. A thermostatic water-circulating bath (CF41, JULABO, Germany) with an uncertainty of ± 0.05 K was selected to control the temperature. To mix the solute and solvent, a magnetic stirrer was used. The solutions were stirred for ten hours. The concentration was confirmed every 0.5 h to determine when solid–liquid equilibrium was reached. After that, the solution was allowed to stand for another four hours without stirring. Approximately 5 mL of the upper clear solution was sampled. A 0.45 μm pore size syringe filter (preheated to the corresponding temperature before use) was utilized to filter the solution.²⁷ All samples were dried in a vacuum drying oven at

Table 2. Experimental and Fitted Solubility Data of IHI in DMF + Water Binary Solvent Mixtures ($P = 0.1$ MPa)^a

T/K	$10^3x_1^{\text{exp}}$	$10^3x_1^{\text{Apelblat}}$	$10^3x_1^{\text{Yaws}}$	$10^3x_1^{\text{Sun}}$	$10^3x_1^{\text{JA}}$	T/K	$10^3x_1^{\text{exp}}$	$10^3x_1^{\text{Apelblat}}$	$10^3x_1^{\text{Yaws}}$	$10^3x_1^{\text{Sun}}$	$10^3x_1^{\text{JA}}$
$x_2^0 = 0.3$						303.15	19.86	19.49	19.53	18.91	19.13
283.15	0.3723	0.4142	0.4145	0.3537	0.3690	308.15	24.64	24.58	24.63	23.89	24.21
288.15	0.5552	0.5943	0.5946	0.5264	0.5560	313.15	30.25	30.57	30.61	29.96	30.31
293.15	0.7951	0.8418	0.8421	0.7728	0.8239	318.15	37.62	37.52	37.53	37.30	37.58
298.15	1.275	1.178	1.178	1.120	1.202	323.15	45.47	45.48	45.43	46.13	46.17
303.15	1.715	1.630	1.630	1.604	1.727	$x_2^0 = 0.8$					
308.15	2.237	2.231	2.231	2.269	2.447	283.15	9.244	8.641	8.604	8.941	8.675
313.15	2.896	3.021	3.021	3.176	3.421	288.15	11.25	11.45	11.43	11.41	11.24
318.15	4.084	4.051	4.051	4.398	4.722	293.15	14.53	14.85	14.86	14.43	14.38
323.15	5.394	5.382	5.383	6.030	6.439	298.15	18.51	18.91	18.92	18.11	18.19
$x_2^0 = 0.4$						303.15	23.76	23.64	23.65	22.56	22.77
283.15	1.192	1.055	1.059	1.284	1.241	308.15	29.21	29.04	29.04	27.90	28.19
288.15	1.657	1.582	1.586	1.833	1.796	313.15	35.13	35.11	35.09	34.28	34.58
293.15	2.294	2.328	2.332	2.584	2.560	318.15	42.06	41.81	41.78	41.84	42.02
298.15	3.239	3.369	3.372	3.600	3.595	323.15	48.85	49.08	49.07	50.75	50.61
303.15	4.737	4.797	4.798	4.963	4.980	$x_2^0 = 0.9$					
308.15	6.813	6.727	6.724	6.771	6.809	283.15	10.67	10.12	10.07	11.15	10.72
313.15	9.139	9.297	9.292	9.145	9.194	288.15	13.23	13.31	13.30	13.89	13.58
318.15	12.91	12.67	12.67	12.24	12.27	293.15	16.84	17.12	17.13	17.18	16.99
323.15	16.96	17.05	17.06	16.23	16.19	298.15	21.17	21.56	21.58	21.09	21.04
$x_2^0 = 0.5$						303.15	26.48	26.60	26.63	25.73	25.77
283.15	2.693	2.584	2.588	2.885	2.755	308.15	32.26	32.22	32.22	31.18	31.27
288.15	3.586	3.582	3.584	3.981	3.857	313.15	38.82	38.32	38.31	37.55	37.59
293.15	4.653	4.933	4.932	5.433	5.323	318.15	44.94	44.83	44.81	44.96	44.79
298.15	6.633	6.750	6.748	7.337	7.246	323.15	51.36	51.62	51.62	53.53	52.93
303.15	9.268	9.180	9.180	9.811	9.738	$x_2^0 = 1.0$					
308.15	12.85	12.41	12.41	13.00	12.93	283.15	11.49	10.98	10.96	13.01	12.63
313.15	16.74	16.69	16.69	17.06	16.96	288.15	14.53	14.30	14.31	15.86	15.64
318.15	21.83	22.32	22.32	22.21	22.01	293.15	17.66	18.23	18.25	19.19	19.16
323.15	29.89	29.69	29.69	28.67	28.27	298.15	22.14	22.76	22.79	23.08	23.23
$x_2^0 = 0.6$						303.15	28.04	27.89	27.91	27.59	27.88
283.15	4.318	4.065	3.997	4.819	4.651	308.15	33.87	33.57	33.56	32.79	33.16
288.15	5.593	5.739	5.690	6.461	6.329	313.15	40.14	39.72	39.70	38.75	39.10
293.15	7.537	7.941	7.916	8.578	8.498	318.15	46.04	46.25	46.24	45.56	45.73
298.15	10.57	10.78	10.78	11.28	11.26	323.15	52.99	53.05	53.09	53.29	53.05
$x_2^0 = 0.7$											
283.15	6.498	6.582	6.499	6.834	6.652						
288.15	8.615	8.856	8.803	8.932	8.825						
293.15	11.74	11.71	11.69	11.57	11.56						
298.15	15.23	15.22	15.24	14.85	14.96						

328.15 K for 12 hours (to constant weight even if a longer drying time was required). A balance (Model AL204, Mettler Toledo, Switzerland) was used to measure all masses with an accuracy of ± 0.0001 g. All experiments were repeated at least three times, and the mole fraction solubility (x_1) of IHI in different solvent systems was calculated based on the following formula^{28,29}

$$x_1 = \frac{m_1 / M_1}{m_1 / M_1 + \sum_{i=2}^n m_i / M_i} \quad (8)$$

where m_1 represents the mass of the solute (IHI); m_i represents the mass of the solvent; M_1 and M_i are the corresponding relative molecular weights, respectively; and N is the amount of solvent. In a pure solvent system, n equals 2, and in a binary solvent system, it equals 3. The initial molar fraction (x_2^0) of a good

solvent (DMF or THF) in a binary solvent system is defined by the following equation

$$x_2^0 = \frac{m_2 / M_2}{m_2 / M_2 + m_3 / M_3} \quad (9)$$

4. RESULTS AND DISCUSSION

4.1. XRPD. The crystal form of IHI was determined by the XRPD method. The XRPD patterns of IHI in different solvents including the residual solids in DMF + water, DMF + ethanol, THF + water, and THF + ethanol in each good solvent compositions and temperatures. The representative data are shown in Figure 2 (take the residual solid under $x_2^0 = 0.6$ as

Table 3. Experimental and Fitted Solubility Data of IHI in DMF + Ethanol Binary Solvent Mixtures ($P = 0.1$ MPa)^a

T/K	$10^3 x_1^{\text{exp}}$	$10^3 x_1^{\text{Apelblat}}$	$10^3 x_1^{\text{Yaws}}$	$10^3 x_1^{\text{Sun}}$	$10^3 x_1^{\text{JA}}$	T/K	$10^3 x_1^{\text{exp}}$	$10^3 x_1^{\text{Apelblat}}$	$10^3 x_1^{\text{Yaws}}$	$10^3 x_1^{\text{Sun}}$	$10^3 x_1^{\text{JA}}$
$x_2^0 = 0.3$						303.15	33.88	33.83	33.82	33.62	33.52
283.15	4.329	4.649	4.640	4.954	5.034	308.15	39.92	39.73	39.75	40.14	40.00
288.15	5.803	5.951	5.944	6.284	6.336	313.15	47.09	46.81	46.84	47.65	47.53
293.15	7.880	7.558	7.553	7.905	7.925	318.15	55.38	55.29	55.30	56.26	56.24
298.15	9.760	9.525	9.524	9.869	9.855	323.15	65.23	65.48	65.41	66.09	66.29
303.15	12.05	11.92	11.92	12.23	12.19	$x_2^0 = 0.8$					
308.15	14.64	14.81	14.81	15.05	14.99	283.15	17.14	16.82	16.84	15.52	15.73
313.15	18.35	18.28	18.28	18.40	18.35	288.15	19.81	19.89	19.88	18.94	19.07
318.15	21.99	22.43	22.42	22.36	22.34	293.15	23.29	23.51	23.49	22.96	23.01
323.15	27.59	27.35	27.33	27.00	27.08	298.15	27.49	27.79	27.77	27.65	27.62
$x_2^0 = 0.4$						303.15	32.93	32.85	32.83	33.10	33.00
283.15	7.091	7.382	7.272	7.635	7.755	308.15	38.82	38.82	38.81	39.38	39.25
288.15	9.022	9.008	8.926	9.575	9.654	313.15	46.01	45.87	45.87	46.61	46.49
293.15	11.06	11.05	11.01	11.92	11.95	318.15	54.36	54.18	54.19	54.86	54.84
298.15	13.65	13.63	13.64	14.72	14.70	323.15	63.79	63.98	63.96	64.25	64.44
303.15	17.27	16.90	16.95	18.06	18.00	$x_2^0 = 0.9$					
308.15	20.91	21.03	21.12	22.01	21.93	283.15	13.88	13.44	13.44	14.39	14.58
313.15	26.09	26.27	26.38	26.65	26.58	288.15	16.71	16.74	16.74	17.52	17.64
318.15	33.22	32.93	32.99	32.08	32.07	293.15	20.14	20.61	20.63	21.19	21.23
323.15	41.28	41.42	41.31	38.40	38.52	298.15	24.97	25.13	25.14	25.46	25.43
$x_2^0 = 0.5$						303.15	30.42	30.34	30.35	30.41	30.32
283.15	10.64	10.59	10.60	10.91	11.08	308.15	36.36	36.31	36.31	36.11	35.99
288.15	12.96	13.02	13.02	13.55	13.65	313.15	43.36	43.07	43.07	42.64	42.54
293.15	16.28	15.96	15.96	16.70	16.74	318.15	50.66	50.67	50.67	50.09	50.08
298.15	19.21	19.53	19.52	20.44	20.41	323.15	59.06	59.15	59.18	58.55	58.73
303.15	23.52	23.85	23.84	24.85	24.77	$x_2^0 = 1.0$					
308.15	29.43	29.05	29.04	30.02	29.91	283.15	11.49	10.98	10.96	13.27	13.43
313.15	35.28	35.31	35.31	36.05	35.95	288.15	14.53	14.30	14.31	16.11	16.21
318.15	42.85	42.83	42.83	43.04	43.02	293.15	17.66	18.23	18.25	19.44	19.47
323.15	51.79	51.83	51.83	51.11	51.27	298.15	22.14	22.76	22.79	23.31	23.28
$x_2^0 = 0.6$						303.15	28.04	27.89	27.91	27.78	27.69
283.15	15.09	15.01	15.02	13.89	14.09	308.15	33.87	33.57	33.56	32.92	32.81
288.15	18.18	18.15	18.15	17.11	17.24	313.15	40.14	39.72	39.70	38.80	38.70
293.15	21.82	21.85	21.85	20.93	20.98	318.15	46.04	46.25	46.24	45.49	45.48
298.15	25.78	26.19	26.19	25.43	25.40	323.15	52.99	53.05	53.09	53.08	53.23
$x_2^0 = 0.7$											
283.15	18.69	18.41	18.41	15.55	15.77						
288.15	21.48	21.31	21.28	19.05	19.18						
293.15	24.25	24.76	24.73	23.17	23.22						
298.15	28.49	28.89	28.87	28.00	27.96						

representative). It is obvious that there is no change in crystal form during the dissolution equilibrium process. The main peaks of the XRD patterns are 7.11, 14.84, 17.92, 18.98, 21.09, 25.14, and 28.58°. There is no difference in peak position and only a slight difference in peak intensity, which indicates that there is no crystal form transformation during the solid–liquid equilibrium process of IHI.

4.2. Solubility Data. In the pre-experiments, more than 20 kinds of pure solvents (such as methanol, ethanol, *n*-propanol, *i*-propanol, *n*-butanol, *i*-butanol, *s*-butanol, *n*-pentanol, *i*-pentanol, 2-butaneone, methyl isobutyl ketone, cyclohexanone, ethyl formate, ethyl acetate, propyl acetate, isopropyl acetate, butyl acetate, amyl acetate, *N,N*-dimethylformamide, tetrahydrofuran, toluene, 1,4-dioxane, etc.) were used for the solubility

measurement of IHI. However, in most of the above solvents, solubility data are almost impossible to measure because IHI dissolves slightly. Thus, in this investigation, DMF and THF were selected as good solvents, while water and ethanol were selected as antisolvents.^{30,31} The mole fraction of good solvent was ranging from 0.3 to 1.0 with an interval of 0.1 in the four binary mixed solvents. The solubilities of IHI in binary solvents are presented in Figure 3.

From Tables 2–5, it can be seen that the solubility of IHI in four binary solvents increases with the increase of temperature. The solubilities of IHI in DMF + water solvents increase with a rise in the mole fraction of DMF and investigated temperature, while for the mixtures of DMF+ ethanol, THF + water, and THF + ethanol, the solubility increased at first and then decreased

Table 4. Experimental and Fitted Solubility Data of IHI in THF + Water Binary Solvent Mixtures ($P = 0.1$ MPa)^a

T/K	$10^3 x_1^{\text{exp}}$	$10^3 x_1^{\text{Apelblat}}$	$10^3 x_1^{\text{Yaws}}$	$10^3 x_1^{\text{Sun}}$	$10^3 x_1^{\text{JA}}$	T/K	$10^3 x_1^{\text{exp}}$	$10^3 x_1^{\text{Apelblat}}$	$10^3 x_1^{\text{Yaws}}$	$10^3 x_1^{\text{Sun}}$	$10^3 x_1^{\text{JA}}$
$x_2^0 = 0.3$						303.15	40.30	40.38	39.66	40.27	40.35
283.15	8.843	8.920	9.505	9.252	8.942	308.15	45.46	45.17	44.89	45.58	45.16
288.15	10.35	10.45	11.23	11.08	10.46	313.15	50.61	50.59	50.86	51.38	50.59
293.15	12.84	12.33	13.23	13.20	12.32	318.15	57.44	56.72	57.67	57.70	56.72
298.15	14.59	14.61	15.56	15.62	14.60	323.15	63.09	63.63	65.45	64.56	63.62
303.15	16.80	17.41	18.25	18.38	17.40	$x_2^0 = 0.8$					
308.15	20.88	20.83	21.35	21.53	20.84	283.15	22.63	22.72	23.2	22.18	22.75
313.15	25.58	25.03	24.93	25.08	25.06	288.15	25.34	25.24	25.93	25.43	25.24
318.15	29.89	30.20	29.05	29.08	30.22	293.15	28.07	28.18	29.05	29.03	28.16
323.15	36.62	36.56	33.77	33.56	36.56	298.15	31.96	31.59	32.62	32.99	31.57
$x_2^0 = 0.4$						303.15	35.35	35.54	36.7	37.33	35.53
283.15	13.32	13.63	14.12	13.69	13.65	308.15	39.93	40.14	41.38	42.08	40.14
288.15	15.81	15.59	16.43	16.20	15.58	313.15	45.53	45.47	46.72	47.25	45.49
293.15	18.17	17.96	19.10	19.05	17.94	318.15	51.75	51.67	52.84	52.86	51.67
298.15	20.86	20.80	22.17	22.29	20.78	323.15	58.82	58.88	59.85	58.93	58.83
303.15	23.97	24.23	25.70	25.94	24.22	$x_2^0 = 0.9$					
308.15	28.59	28.37	29.75	30.05	28.37	283.15	16.23	16.69	17.22	16.40	16.70
313.15	33.24	33.36	34.40	34.64	33.37	288.15	19.03	18.74	19.19	18.80	18.74
318.15	39.21	39.40	39.72	39.75	39.41	293.15	21.49	21.17	21.45	21.45	21.16
323.15	46.84	46.72	45.80	45.42	46.68	298.15	23.97	24.02	24.05	24.36	24.02
$x_2^0 = 0.5$						303.15	27.83	27.38	27.04	27.56	27.40
283.15	19.16	18.83	18.54	17.91	19.07	308.15	30.92	31.35	30.48	31.05	31.37
288.15	21.64	21.43	21.3	20.98	21.54	313.15	35.75	36.02	34.43	34.85	36.05
293.15	24.34	24.45	24.47	24.43	24.46	318.15	41.64	41.53	38.97	38.97	41.55
298.15	27.83	27.99	28.11	28.30	27.92	323.15	48.13	48.04	44.19	43.43	48.01
303.15	31.89	32.12	32.27	32.64	32.00	$x_2^0 = 1.0$					
308.15	36.61	36.94	37.02	37.46	36.82	283.15	7.294	7.202	8.687	8.240	7.202
313.15	42.71	42.57	42.46	42.80	42.48	288.15	8.352	8.308	9.717	9.510	8.297
318.15	49.52	49.15	48.67	48.71	49.15	293.15	9.424	9.602	10.91	10.91	9.587
323.15	56.72	56.85	55.76	55.20	56.99	298.15	11.04	11.12	12.29	12.47	11.10
$x_2^0 = 0.6$						303.15	12.86	12.90	13.89	14.18	12.88
283.15	24.46	24.23	22.34	21.51	24.26	308.15	15.04	14.98	15.75	16.07	14.98
288.15	27.39	27.12	25.38	24.96	27.12	313.15	17.41	17.42	17.89	18.13	17.42
293.15	29.84	30.39	28.86	28.82	30.38	318.15	20.46	20.28	20.38	20.38	20.29
298.15	33.75	34.11	32.84	33.12	34.10	323.15	23.53	23.63	23.26	22.82	23.64
303.15	38.45	38.32	37.38	37.88	38.32						
308.15	43.43	43.10	42.57	43.14	43.11						
313.15	48.35	48.52	48.49	48.93	48.54						
318.15	55.12	54.66	55.24	55.28	54.68						
323.15	61.33	61.62	62.95	62.21	61.63						
$x_2^0 = 0.7$											
283.15	26.39	26.11	24.50	23.50	26.14						
288.15	29.33	29.05	27.57	27.08	29.04						
293.15	31.93	32.37	31.08	31.05	32.35						
298.15	35.54	36.13	35.09	35.44	36.10						

with the increasing mass fraction of DMF or THF at a given temperature. That is to say, there is a co-solvency phenomenon in these three mixed solvents (DMF + ethanol, THF + water, and THF + ethanol). The maximum solubility occurred with the mole fraction of good solvent at $x_2^0 = 0.7$ (DMF + ethanol), 0.7 (THF + water), and 0.8 (THF + ethanol) at a given temperature, respectively. The co-solvency phenomenon has important guiding significance for the selection of initial concentration in the process of industrial crystallization. At a given temperature and solvent ratio, the solubility sequence of IHI is basically consistent as DMF + ethanol \geq THF + water \geq DMF + water \geq THF + ethanol. The effect of solvent polarity on solubility is not obvious here. Solubility is affected by many factors. The intermolecular interactions such as hydrogen bonds

and van der Waals forces between solvent–solvent and solute–solvent will also influence the solubility.

The maximum solubility of IHI exists in the solvent of DMF + ethanol ($0.06523 \text{ mol}\cdot\text{mol}^{-1}$, $x_2^0 = 0.7$, $T = 323.15 \text{ K}$), while the minimum solubility exists in DMF + water ($0.0003723 \text{ mol}\cdot\text{mol}^{-1}$, $x_2^0 = 0.3$, $T = 283.15 \text{ K}$). The maximum solubility value is approximately 175 times than the minimum solubility value. Except for the solvent DMF + water, the theoretical molar yield of each binary mixed solvent ranges from 58 to 84% with cooling conditions ranging from 323.15 to 283.15 K. The theoretical molar yield of the antisolvent method is 80% in all of the selected solvent systems. The solvent composition is more sensitive to solubility than temperature changes. In addition, when the cooling and antisolvent methods were combined, the theoretical

^a x_1^{exp} is the experimental solubility of IHI in THF + water binary solvent system, and x_2^0 denotes the initial mole fraction of DMF in the binary solvent mixture. x_1^{Apelblat} , x_1^{Yaws} , x_1^{Sun} , and x_1^{JA} represent the calculated solubilities using the modified Apelblat model, Yaws model, Sun model, and modified Jouyban–Acree model, respectively. The standard uncertainty of temperature is $u(T) = 0.05 \text{ K}$, and the relative standard uncertainty of pressure is $u(P) = 0.05$. The relative standard uncertainty of mole fraction solubility is $u_r(x_1) = 0.03$, and the relative standard uncertainty of the solvent composition is $u_r(x_2^0) = 0.0002$.

Table 5. Experimental and Fitted Solubility Data of IHI in THF + ethanol Binary Solvent Mixtures ($P = 0.1$ MPa)^a

T/K	$10^3x_1^{exp}$	$10^3x_1^{Apelblat}$	$10^3x_1^{Yaws}$	$10^3x_1^{Sun}$	$10^3x_1^{JA}$	T/K	$10^3x_1^{exp}$	$10^3x_1^{Apelblat}$	$10^3x_1^{Yaws}$	$10^3x_1^{Sun}$	$10^3x_1^{JA}$
$x_2^0 = 0.3$						303.15	19.19	19.11	19.29	19.38	19.12
283.15	5.132	5.204	4.905	4.860	5.210	308.15	21.79	21.65	21.94	22.04	21.67
288.15	6.023	5.914	5.721	5.696	5.913	313.15	24.29	24.57	24.88	24.96	24.59
293.15	6.711	6.736	6.645	6.641	6.733	318.15	27.78	27.93	28.15	28.16	27.94
298.15	7.795	7.689	7.689	7.703	7.686	323.15	31.98	31.79	31.77	31.64	31.78
303.15	8.686	8.793	8.864	8.890	8.792	$x_2^0 = 0.8$					
308.15	9.931	10.07	10.18	10.21	10.08	283.15	12.18	12.50	11.63	11.46	12.51
313.15	11.69	11.55	11.66	11.68	11.56	288.15	14.03	14.00	13.36	13.28	14.00
318.15	13.32	13.27	13.30	13.30	13.28	293.15	16.07	15.72	15.31	15.31	15.71
323.15	15.23	15.27	15.14	15.09	15.27	298.15	17.73	17.67	17.50	17.56	17.67
$x_2^0 = 0.4$						303.15	20.19	19.91	19.95	20.05	19.91
283.15	6.458	6.489	6.433	6.374	6.501	308.15	22.39	22.46	22.68	22.80	22.47
288.15	7.460	7.357	7.468	7.441	7.357	313.15	24.99	25.37	25.73	25.83	25.39
293.15	8.285	8.383	8.637	8.641	8.377	318.15	28.48	28.69	29.12	29.13	28.71
298.15	9.564	9.596	9.953	9.984	9.588	323.15	32.78	32.49	32.88	32.74	32.48
303.15	11.07	11.03	11.43	11.48	11.03	$x_2^0 = 0.9$					
308.15	12.88	12.72	13.08	13.14	12.73	283.15	10.79	10.95	10.40	10.25	10.98
313.15	14.55	14.73	14.93	14.98	14.74	288.15	12.33	12.27	11.98	11.90	12.28
318.15	17.14	17.11	16.99	17.00	17.12	293.15	13.92	13.82	13.76	13.76	13.81
323.15	19.95	19.93	19.27	19.23	19.93	298.15	15.69	15.63	15.76	15.82	15.62
$x_2^0 = 0.5$						303.15	17.96	17.74	18.00	18.11	17.74
283.15	8.321	8.294	8.130	8.044	8.294	308.15	20.21	20.23	20.52	20.64	20.23
288.15	9.377	9.409	9.400	9.359	9.398	313.15	22.87	23.13	23.32	23.42	23.15
293.15	10.73	10.70	10.83	10.83	10.69	318.15	26.41	26.55	26.46	26.48	26.56
298.15	12.19	12.21	12.44	12.48	12.19	323.15	30.74	30.55	29.95	29.82	30.55
303.15	13.81	13.96	14.24	14.30	13.95	$x_2^0 = 1.0$					
308.15	16.06	15.99	16.25	16.33	15.99	283.15	7.294	7.202	7.550	7.421	7.202
313.15	18.32	18.36	18.49	18.55	18.36	288.15	8.352	8.308	8.740	8.673	8.297
318.15	21.27	21.11	20.99	21.00	21.12	293.15	9.424	9.602	10.09	10.08	9.587
323.15	24.23	24.31	23.75	23.68	24.31	298.15	11.04	11.12	11.62	11.66	11.10
$x_2^0 = 0.6$						303.15	12.86	12.90	13.35	13.43	12.88
283.15	9.886	10.17	9.853	9.735	10.18	308.15	15.04	14.98	15.30	15.38	14.98
288.15	11.62	11.52	11.36	11.30	11.52	313.15	17.41	17.42	17.48	17.55	17.42
293.15	13.44	13.06	13.04	13.04	13.06	318.15	20.46	20.28	19.94	19.94	20.29
298.15	14.97	14.85	14.94	14.98	14.84	323.15	23.53	23.63	22.69	22.57	23.64
$x_2^0 = 0.7$											
283.15	11.58	11.85	11.23	11.08	11.86						
288.15	13.43	13.31	12.91	12.84	13.30						
293.15	15.27	14.98	14.80	14.80	14.97						
298.15	16.83	16.90	16.92	16.97	16.90						

molar yield can reach higher than 88%. What should be especially mentioned is that, in the solvent of DMF + water, when using the cooling method with the antisolvent method, the theoretical molar yield can reach more than 99%.

4.3. Data Correlation. Parameters, RADs, and RMSDs values of the selected model in this article are listed in Tables 6–9. All of the RAD values are less than 0.0484 (Sun model, DMF + water), and RMSD values are no more than 0.001319 (Sun model, THF + water). Considering the RAD values, the fitting order of the selected four thermodynamic models is Yaws \geq modified Apelblat \geq Sun \geq modified Jouyban–Acree. Considering the RMSD values, the fitting order of the selected four thermodynamic models is modified Apelblat \geq Yaws \geq modified Jouyban–Acree \geq Sun. The Yaws model and the

modified Apelblat model fit the solubility data of IHI better than the other two models. All in all, all of the selected four models can fit the solubility data of IHI well.

5. CONCLUSIONS

The solubility of IHI in four commonly used binary solvent mixtures of *N,N*-dimethylformamide (DMF) + water, DMF + ethanol, tetrahydrofuran (THF) + water, and THF + ethanol was determined with the gravimetric method at temperatures ranging from 283.15 to 323.15 K under atmospheric pressure. The solubility of IHI in all selected solvents increases with the increase of temperature. There is a co-solvency phenomenon in the mixed solvents of DMF+ ethanol, THF + water, and THF + ethanol. The maximum solubility of IHI exists in the solvent of

Table 6. Parameters of the Modified Apelblat Model for IHI in Binary Solvent Mixtures^a

x_2^0	A_1	B_2	C_3	100 RAD	10^4 RMSD
DMF + water					
0.3	22.5674	6300.0844	-14.4358	4.71	0.66
0.4	111.3980	10677.0421	-14.2657	3.13	1.27
0.5	-89.8601	-918.8117	15.4352	2.17	2.62
0.6	202.3326	13696.3584	-28.2443	2.30	2.54
0.7	181.0354	12095.6740	-25.3881	0.87	1.88
0.8	257.4723	15147.7968	-36.9690	1.65	3.03
0.9	311.3921	17362.2711	-45.1060	1.32	3.14
1.0	293.8373	16462.8750	-42.5448	1.68	3.89
average				2.23	2.38
DMF + ethanol					
0.3	-0.1104	-3645.7022	1.3487	2.43	2.54
0.4	-272.2591	8719.3702	41.8982	1.01	2.04
0.5	-98.1654	1159.4091	15.8560	0.83	2.41
0.6	-34.9823	-1312.0190	6.2729	0.64	2.94
0.7	-203.4855	6541.5136	31.2414	0.84	2.82
0.8	-125.2021	2883.5480	19.6482	0.61	1.95
0.9	83.0580	-6783.9999	-11.2307	0.84	0.25
1.0	293.8373	16462.8750	-42.5448	1.68	3.89
average				1.11	2.36
THF + water					
0.3	-250.4788	8351.1064	38.3044	1.46	3.42
0.4	-244.5529	8447.3423	37.2697	0.90	2.04
0.5	-164.3752	5096.3882	25.2222	0.74	2.52
0.6	-116.8804	3299.5604	17.9787	0.84	3.35
0.7	-116.4081	3363.4658	17.8683	0.89	4.22
0.8	-181.0344	6148.4414	27.5480	0.42	1.70
0.9	-205.5813	7037.6446	31.2848	1.14	3.13
1.0	-151.6913	4321.7412	23.2900	0.72	1.03
average				0.89	2.68
THF + ethanol					
0.3	-147.8303	4348.9300	22.5316	1.04	0.96
0.4	-204.8489	6837.1695	31.1132	0.73	0.96
0.5	-158.2689	4841.3186	24.1550	0.44	0.85
0.6	-136.9302	3963.4145	20.9609	1.09	1.91
0.7	-144.5506	4410.9687	22.0577	0.99	1.94
0.8	-131.9881	3908.2125	20.1566	1.13	2.55
0.9	-194.7470	6591.9896	29.5701	0.74	1.55
1.0	-151.6913	4321.7412	23.2900	0.72	1.03
average				0.86	1.47

DMF + ethanol ($0.06523 \text{ mol} \cdot \text{mol}^{-1}$, $x_2^0 = 0.7$, $T = 323.15 \text{ K}$), while the minimum solubility exists in DMF + water ($0.0003723 \text{ mol} \cdot \text{mol}^{-1}$, $x_2^0 = 0.3$, $T = 283.15 \text{ K}$). Four thermodynamic models including the modified Apelblat model, the Yaws model, the Sun model, and the modified Jouyban–Acree model were selected to fit the solubility data of IHI. The Yaws model and the modified Apelblat model fit the solubility data of IHI better than the other two models. All in all, all of the selected four models can fit the solubility data of IHI well.

■ AUTHOR INFORMATION

Corresponding Authors

Yuanxing Cai — School of Material Science and Engineering, Shandong Jianzhu University, Jinan 250101, P. R. China; Email: caiyuanxing@163.com

Fumin Xue — School of Pharmaceutical Sciences (Shandong Analysis and Test Center), Qilu University of Technology

(Shandong Academy of Sciences), Jinan 250014, P. R. China;  orcid.org/0000-0002-8097-0108; Email: xuefumin@qlu.edu.cn

Authors

Qi Dong — School of Material Science and Engineering, Shandong Jianzhu University, Jinan 250101, P. R. China; School of Pharmaceutical Sciences (Shandong Analysis and Test Center), Qilu University of Technology (Shandong Academy of Sciences), Jinan 250014, P. R. China

Shuai Yu — School of Pharmaceutical Sciences (Shandong Analysis and Test Center), Qilu University of Technology (Shandong Academy of Sciences), Jinan 250014, P. R. China;  orcid.org/0000-0001-9249-2513

Xingzhu Wang — School of Pharmaceutical Sciences (Shandong Analysis and Test Center), Qilu University of Technology (Shandong Academy of Sciences), Jinan 250014, P. R. China

Shangzhi Ding — School of Pharmaceutical Sciences (Shandong Analysis and Test Center), Qilu University of Technology (Shandong Academy of Sciences), Jinan 250014, P. R. China

Enxia Li — School of Pharmaceutical Sciences (Shandong Analysis and Test Center), Qilu University of Technology (Shandong Academy of Sciences), Jinan 250014, P. R. China

Complete contact information is available at:

<https://pubs.acs.org/10.1021/acsomega.3c04987>

Author Contributions

[§]Q.D. and S.Y. contributed equally to this work and should be regarded as co-first authors.

Notes

The authors declare no competing financial interest.

■ ACKNOWLEDGMENTS

This investigation work received support from the Shandong Provincial Natural Science Foundation (grant reference: ZR2023MB036, and ZR2020QB177), Central Guidance on Local Science and Technology Development Fund of Shandong Province (grant references: YDZX2021054, and YDZX2022098), the National Natural Science Foundation of China (grant reference: 82204288), Shandong Keypoint Research & Development Plan (grant references: 2021CXGC010514, and 2021CXGC010811), and Science, Education and Industry Integration Technology Innovation Project (grant references: 2022PX036, and 2022PT117).

■ REFERENCES

- Liang, X.; Van Parys, M.; Ding, X.; Zeng, N.; Bi, L.; Dorshort, D.; McKnight, J.; Milanowski, D.; Mao, J.; Chen, Y.; Ware, J. A.; Dean, B.; Hop, C. E. C. A.; Deng, Y. Simultaneous determination of itraconazole, hydroxy itraconazole, keto itraconazole and N-desalkyl itraconazole concentration in human plasma using liquid chromatography with tandem mass spectrometry. *J. Chromatogr. B* **2016**, *1020*, 111–119.
- Wang, J.; Li, F.; Lakerveld, R. Process intensification for pharmaceutical crystallization. *Chem. Eng. Process.* **2018**, *127*, 111–126.
- Duan, J.; Chen, L.; Hong, R.; Li, Y.; Huang, J. Efficient crystallization process of dodecanedioic acid by a pneumatically agitated crystallizer. *Prep. Biochem. Biotechnol.* **2023**, *1*–8.
- Leng, Y.; Qi, H. Solubility of aspartame in water, methanol, ethanol and different binary mixtures in the temperature range of (278.15 to 333.15) K. *J. Chem. Eng. Data* **2014**, *59*, 1549–1555.
- Yu, S.; Cheng, Y.; Xing, W.; Xue, F. Solubility determination and thermodynamic modelling of gliclazide in five binary solvent mixtures. *J. Mol. Liq.* **2020**, *311*, No. 113258.

- (6) Yu, S.; Gao, X.; Ge, S.; Ma, Y.; Han, Y.; Wang, X.; Xue, F.; Fu, L. Equilibrium solubility, thermodynamic modelling and Hansen solubility parameters of glimepiride (form I) in binary solvent mixtures at various temperatures. *J. Mol. Liq.* **2023**, *372*, No. 121230.
- (7) Zhan, N.; Zhang, Y.; Wang, X. Z. Solubility of N-tert-Butylbenzothiazole-2-sulfenamide in several pure and binary solvents. *J. Chem. Eng. Data* **2019**, *64*, 1051–1062.
- (8) Zhao, H.-K.; Ji, H.-Z.; Meng, X.-c.; Li, R.-R. Solubility of 3-chlorophthalic anhydride and 4-chlorophthalic anhydride in organic solvents and solubility of 3-chlorophthalic acid and 4-chlorophthalic acid in water from (283.15 to 333.15) K. *J. Chem. Eng. Data* **2009**, *54*, 1135–1137.
- (9) Shakeel, F.; Bhat, M. A.; Haq, N.; Fathi-Azarbayjani, A.; Jouyban, A. Solubility and thermodynamic parameters of a novel anti-cancer drug (DHP-5) in polyethylene glycol 400+water mixtures. *J. Mol. Liq.* **2017**, *229*, 241–245.
- (10) Zhang, F.; Tang, Y.; Wang, L.; Xu, L.; Liu, G. Solubility determination and thermodynamic models for 2-methylnaphthalene in different solvents from $T = (278.15 \text{ to } 303.15)$ K. *J. Chem. Eng. Data* **2015**, *60*, 1699–1705.
- (11) Zhang, L.; Huang, C. Study on 6-Bromo-2-methylquinoline in ten monosolvents and four binary blends at 278.15 – 323.15 K: Solubility, correlation, and solvent effect. *J. Chem. Eng. Data* **2023**, *68*, 1253–1264.
- (12) Apelblat, A.; Manzurola, E. Solubilities of L-aspartic, DL-aspartic, DL-glutamic, p-hydroxybenzoic, o-anisic, p-anisic, and itaconic acids in water from $T = 278$ K to $T = 345$ K. *J. Chem. Thermodyn.* **1997**, *29*, 1527–1533.
- (13) Gao, X.; Yu, S.; Zhang, G.; Cheng, Y.; Wang, S.; Xue, F. Solid–liquid equilibrium, thermodynamic modelling and the solvent effect of glimepiride in mono-solvents and binary mixed solvents. *J. Mol. Liq.* **2022**, *360*, No. 119402.
- (14) Jouyban, A. Review of the cosolvency models for predicting solubility of drugs in water-cosolvent mixtures. *J. Pharm. Pharm. Sci.* **2008**, *11*, 32–58.
- (15) Yu, C.; Sun, X.; Wang, Y.; Du, S.; Shu, L.; Sun, Q.; Xue, F. Determination and correlation of solubility of metformin hydrochloride in aqueous binary solvents from 283.15 to 323.15 K. *ACS Omega* **2022**, *7*, 8591–8600.
- (16) Gao, X.; Yu, S.; Wu, G.; Cheng, Y.; Xue, F. Solid–liquid phase equilibrium of 2-mercapto-1,3,4-thiadiazol in pure organic solvents. *J. Chem. Eng. Data* **2021**, *66*, 4706–4713.
- (17) Alyamani, M.; Alshehri, S.; Alam, P.; Ud Din Wani, S.; Ghoneim, M. M.; Shakeel, F. Solubility and solution thermodynamics of raloxifene hydrochloride in various (DMSO + water) compositions. *Alexandria Eng. J.* **2022**, *61*, 9119–9128.
- (18) Bhola, R.; Ghumara, R.; Patel, C.; Parsana, V.; Bhatt, K.; Kundariya, D.; Vaghani, H. Solubility and thermodynamics profile of benzethonium chloride in pure and binary solvents at different temperatures. *ACS Omega* **2023**, *8*, 14430–14439.
- (19) Wang, Z.; Yu, S.; Li, H.; Liu, B.; Xia, Y.; Guo, J.; Xue, F. Solid–liquid equilibrium behavior and solvent effect of gliclazide in mono- and binary solvents. *ACS Omega* **2022**, *7*, 37663–37673.
- (20) Ma, Y.; Gao, Y.; Gao, X.; Wang, Z.; Feng, W.; Xing, W.; Li, H.; Yu, S.; Xue, F. Measurement and correlation of the solubility of 2-mercapto-1,3,4-thiadiazol in aqueous binary solvent mixtures. *J. Chem. Eng. Data* **2022**, *67*, 775–785.
- (21) Yu, S.; Xing, W.; Xue, F.; Cheng, Y.; Li, B. Solubility and thermodynamic properties of nimodipine in pure and binary solvents at a series of temperatures. *J. Chem. Thermodyn.* **2021**, *152*, No. 106259.
- (22) Kang, X.; Li, M.; Li, J.; Wang, K.; Han, D.; Gong, J. Solubility measurement and thermodynamic correlation of 4-(hydroxymethyl) benzoic acid in nine pure solvents and two binary solvent mixtures at (283.15 – 323.15) K. *J. Chem. Eng. Data* **2021**, *66*, 2114–2123.
- (23) Li, Y.; Zhang, Y.; Wang, X. Z. Solubility of dimethyl 2,2'-Azobis(2-methylpropionate) in 15 pure solvents and in a methanol + water binary solvent system. *J. Chem. Eng. Data* **2020**, *65*, 1411–1424.
- (24) Zhao, L.; Zhang, B.; Xu, L. Solubility behavior of 2-chloro-3-(trifluoromethyl)pyridine in (ethyl acetate + n-butanol, DMF + n-butanol, DMF + ethanol) solvent Mixtures. *J. Chem. Eng. Data* **2019**, *64*, 1085–1094.
- (25) Wu, Y.; Shi, H.; Xie, Y.; Zhu, J.; Wang, C.; Wang, H. Solubility measurement and correlation of pazopanib in (ethanol/n-propanol/2-propanol/1-butanol + acetonitrile) mixtures from $T = 288.15$ to 328.15 K. *J. Chem. Eng. Data* **2022**, *67*, 2583–2589.
- (26) Wilson, G. M. Vapor-liquid equilibrium. XI. A new expression for the excess free energy of mixing. *J. Am. Chem. Soc.* **1964**, *86*, 127–130.
- (27) Wen, T.; Wang, X.; Lu, D. Measurement and correlation of the solubility of salbutamol in ten pure and binary mixed organic solvents from $T = 283.15 – 328.15$ K. *J. Chem. Eng. Data* **2022**, *67*, 3690–3699.
- (28) Jouyban, A.; Fakhree, M. A. A.; Acree, W. E., Jr. Comment on “Measurement and Correlation of Solubilities of (Z)-2-(2-Amino-thiazol-4-yl)-2-methoxyiminoacetic Acid in Different Pure Solvents and Binary Mixtures of Water + (Ethanol, Methanol, or Glycol)”. *J. Chem. Eng. Data* **2012**, *57*, 1344–1346.
- (29) Yu, S.; Yuan, J.; Cheng, Y.; Du, S.; Wang, Y.; Xue, F.; Xing, W. Solid-liquid phase equilibrium of clozapine in aqueous binary solvent mixtures. *J. Mol. Liq.* **2021**, *329*, No. 115371.
- (30) Yang, G.; Fang, S.; Zhang, J.; Wang, R.; Liu, R.; Xu, R.; Huang, C. Solubility measurement and correlation of 2-Amino-3-chloropyrazine and 2-Amino-3,5-dibromopyrazine in a series of mixed solvent systems at $T = (278.15 \text{ to } 323.15)$ K. *J. Chem. Eng. Data* **2022**, *67*, 3186–3200.
- (31) Du, C.; Luo, Y.; Huang, C.; Li, R. Solubility measurement and thermodynamic model correlation of baclofen in 12 pure organic solvents. *J. Chem. Eng. Data* **2022**, *67*, 2655–2661.

Table 7. Parameters of the Yaws Model for IHI in Binary Solvent Mixtures^a

x_2^0	E	F	G	100 RAD	10^4 RMSD
DMF + water					
0.3	12.2847	-5477.0572	-58510.4966	4.72	0.66
0.4	8.7927	-2227.6943	-623436.3669	3.10	1.27
0.5	21.6593	-10374.2692	723389.6447	2.14	2.55
0.6	-3.6129	4770.9081	-1503950.0617	2.33	2.52
0.7	-3.9627	4425.6486	-1339183.8988	0.66	1.78
0.8	-9.7620	7580.5954	-1745056.1789	1.70	3.14
0.9	-14.6948	10389.4395	-2132322.7153	1.40	3.31
1.0	-13.3147	9455.1423	-1971594.9422	1.72	4.02
average				2.22	2.41
DMF + ethanol					
0.3	9.3546	-4299.8374	36725.4325	2.41	2.54
0.4	27.3784	-15050.0483	1671630.1098	0.99	1.91
0.5	16.4720	-8601.2413	750303.6222	0.81	2.26
0.6	10.3187	-5141.7090	291959.5130	0.64	2.93
0.7	21.7350	-12290.4383	1417173.5731	0.81	2.64
0.8	16.7583	-9153.2231	920744.3453	0.58	1.83
0.9	2.0512	12.8836	-513592.2951	0.86	2.52
1.0	-13.3147	9455.1423	-1971594.9422	1.72	4.02
average				1.10	2.58
THF + water					
0.3	26.1017	-15009.0456	1778952.7732	1.48	3.39
0.4	24.4614	-14223.9309	1722057.3704	0.96	2.15
0.5	20.0187	-11680.2372	1384829.3937	0.49	2.00
0.6	12.9774	-7689.6051	838717.4450	0.82	3.28
0.7	12.6826	-7576.9785	836426.9433	0.86	4.12
0.8	17.7787	-10592.3306	1270508.1810	0.42	1.73
0.9	19.9980	-11848.7988	1423551.8673	1.16	3.19
1.0	-13.3147	9455.1423	-1971594.9422	0.68	0.98
average				0.86	2.61
THF + ethanol					
0.3	14.8295	-9371.8146	1043194.4387	1.05	0.97
0.4	19.8265	-12149.8137	1446915.8547	0.72	0.96
0.5	16.1600	-9895.8537	1122192.4710	0.40	0.80
0.6	14.2763	-8731.3099	959908.4919	1.13	1.96
0.7	14.5356	-8928.2408	1007115.0780	1.01	2.01
0.8	13.335	-8249.8836	915551.3089	1.17	2.65
0.9	18.8343	-11483.2133	1379738.0820	0.79	1.64
1.0	-13.3147	9455.1423	-1971594.9422	0.68	0.98
Average				0.87	1.50

Table 8. Parameters of the Sun Model for IHI in Binary Solvent Mixtures

parameters	DMF + water	DMF + ethanol	THF + water	THF + ethanol	average
A_1	18.3570	9.0364	6.7092	3.7187	
A_2	-10091.9754	-4329.7198	-4062.1280	-2912.2647	
A_3	-11.3094	-2.1572	-3.2787	0.3646	
A_4	17709.6379	611.4711	5881.1666	1588.5918	
A_5	-24248.9096	4973.8211	-10113.4012	-2507.9924	
A_6	19342.9012	-7604.7556	11243.5788	3110.1740	
A_7	-5936.5594	3177.4279	-5279.2760	-1823.1146	
100 RAD	4.84	3.73	4.09	2.38	3.76
10^4 RMSD	7.27	9.62	13.19	4.20	8.57

Table 9. Parameters of the Modified Jouyban–Acree Model for IHI in Binary Solvent Mixtures

parameters	DMF + water	DMF + ethanol	THF + water	THF + ethanol	average
A_1	68.8139	-32.6042	-24.1136	-13.7357	
A_2	-12053.4224	-2427.8886	-2644.7130	-2108.8953	
A_3	-7.4778	6.1879	4.5754	2.5957	
A_4	21.5197	7.6931	-143.8933	-32.2577	
A_5	13836.4102	167.8674	12250.2571	3006.3646	
A_6	-18758.9719	4951.2611	10116.9373	-2345.4093	
A_7	14004.9985	-7581.2933	11247.8913	2940.2240	
A_8	-4054.0639	3168.5933	-5281.0276	-1759.4633	
A_9	-4.9018	-1.4623	20.9284	4.8521	
100 RAD	4.23	3.78	4.03	2.10	3.54
10^4 RMSD	6.42	9.47	11.86	3.72	7.87